Tripodal trisamides based on nicotinic and picolinic acid derivatives

H.R. Hoveyda, Veranja Karunaratne, Christopher J. Nichols, Steven J. Rettig, Ashley K.W. Stephens, and Chris Orvig

Abstract: A number of polydentate arylamide ligands have been prepared by coupling various acyclic tripodal or linear polyamines with derivatives of nicotinic and picolinic acids. Two synthetic procedures were utilized; tris{[(2-hydroxynicotinyl)carbonyl]-2-aminoethyl}amine (H_3NICTREN) was prepared by Method A, the HOSu/DCC method, and the other arylamides in this study were prepared by Method B, the CDI method. Method A involved the reaction of N-hydroxysuccinimide with 2-hydroxynicotinic acid (in the presence of dicyclohexylcarbodiimide (DCC) as a dehydrative coupling reagent) to form the succinimide ester, followed by reaction with TREN to yield H_3NICTREN. Method B involved reaction of a carboxylic acid (2-hydroxynicotinic, 3-hydroxypicolinic, nicotinic, or picolinic acids) with carbonyldiimidazole (CDI) to form the N-acylimidazolide, followed by reaction with the amine (TREN, TAME, spermidine, or TRPN) to yield the desired arylamide. The X-ray structure of 1,1,1-tris{[(3-hydroxypicolinyl)carbonyl]-2-aminomethyl}ethane (H_3PICTAME) was determined; crystals of H_3PICTAME are monoclinic, $a = 10.257(2)$, $b = 15.572(3)$, $c = 15.208(2)$ Å, $\beta = 96.124(15)°$, $Z = 4$, space group $P2_1/a$. The structure was solved by direct methods and refined by full-matrix least-squares procedures to $R = 0.041$ and $R_w = 0.038$ for 2506 reflections with $I \geq 3\sigma(I)$. In the solid state, H_3PICTAME contains an extensive hydrogen-bonding network, with eight intra- and one intermolecular H-bonds per molecule; the ligand is partially preorganized for metal ion chelation. The acid dissociation constants of H_3NICTREN and those of 1,1,1-tris{[(2-hydroxynicotinyl)carbonyl]-2-aminomethyl}ethane (H_3NICTAME) have been determined; $pK_{a1} = 11.2$ (10.68), $pK_{a2} = 10.7$ (10.58), $pK_{a3} = 10.0$ (9.71), and $pK_{a4} = 6.25$ for H_3NICTREN (H_3NICTAME); the high phenolic pK_a's are consistent with the hydrogen bonding observed in the solid state.

Key words: arylamide, hydrogen bonding, preorganization.

Résumé : On a préparé une série de ligands arylamides polydentates en procédant au couplage de diverses polyamines linéaires ou acycliques tripodaux avec des dérivés des acides nicotinique et picolinique. On a fait appel à deux voies de synthèse : on a préparé la tris{[(2-hydroxynicotinyl)carbonyl]-2-aminoéthyl}amine (H_3NICTREN) par la méthode A, la méthode au HOSu/DCC, alors que les autres arylamides examinés dans cette étude ont été préparés par la méthode B, la méthode CDI. La méthode A implique la réaction du N-hydroxysuccinimide avec l'acide 2-hydroxynicotinique (en présence de dicyclohexylcarbodiimide (DCC) comme agent de couplage déshydratant) qui conduit à l'ester succinimide, suivie d'une réaction avec du « TREN » pour obtenir le H_3NICTREN. La méthode B implique la réaction d'un acide carboxylique (acides 2-hydroxynicotinique, 3-hydroxypicolinique, nicotinique ou picolinique) avec le carbonyldiimidazole (CDI) pour former le N-acylimidazolide, suivie d'une réaction avec l'amine (« TREN », « TAME », spermidine ou « TRPN ») conduisant à l'arylamide désiré. On a déterminé la structure cristalline du 1,1,1-tris{[(3-hydroxypicolinyl)carbonyl]-2-aminométhyl}éthane (H_3PICTAME). Les cristaux sont monocliniques, groupe d'espace $P2_1/a$, avec $a = 10,257(2)$, $b = 15,572(3)$ et $c = 15,208(2)$ Å, $\beta = 96,124(15)°$ et $Z = 4$. On a résolu la structure par des méthodes directes et on l'a affinée par la méthode des moindres carrés (matrice entière) jusqu'à des valeurs de $R = 0,041$ et $R_w = 0,038$ pour 2506 réflexions avec $I \geq 3\sigma(I)$. À l'état solide, le H_3PICTAME comporte un important réseau de liaisons hydrogènes, avec huit liaisons intra- et une liaison intermoléculaire par molécule; le ligand est partiellement préorganisé pour donner une chélation avec le métal. On a déterminé les constantes de dissociation acide du H_3NICTREN et du 1,1,1-tris{[(3-hydroxypicolinyl)carbonyl]-2-aminométhyl}éthane (H_3PICTAME) qui sont respectivement : $pK_{a1} = 11,2$ (10,68), $pK_{a2} = 10,7$ (10,58), $pK_{a3} = 10,0$ (9,71) et $pK_{a4} = 6,25$; les valeurs élevées du pK_a des phénols sont en accord avec les liaisons hydrogènes observées à l'état solide.

Mots clés : arylamide, liaison hydrogène, préorganisation.

[Traduit par la rédaction]

Introduction

In searching for new ligands to be used in the sequestration of trivalent metal ions (e.g., group 13 and lanthanides), much insight can be gained from an examination of naturally occurring ring chelating agents for trivalent iron. The physical and chemical similarities between Fe(III) and group 13 metals, especially Ga(III), are rather pronounced; they share the same charge and similar ionic radii, e.g., 0.645 Å for Fe(III) compared to 0.620 Å for Ga(III) (1). In addition, the electronic configuration of (aqueous) ferric ion is high-spin d^5, while the group 13 metal ions are diamagnetic (Al(III), d^0; Ga(III) and In(III), d^{10}), and, accordingly, none of these metal ions or the lanthanides are perturbed by crystal field effects (2). The kinship between Ga(III) and Fe(III) is nicely reflected in the kinetics of ligand exchange, for instance, the first-order water exchange rates for Ga(III) and Fe(III) (at 298 K) are 4.0×10^2 and 1.6×10^2 s^{-1}, respectively (3). Also, microorganisms and plants have evolved a host of low-molecular-weight ligands; the *siderophores* (for a general overview, see ref. 4), which show both a high affinity and a high specificity for Fe(III) (formation constants ranging from 10^{25} to 10^{49}) (5). Therefore, in a biomimetic approach, the knowledge gained from ferric ion transport can be applied, for example, to the development of ^{67}Ga radiopharmaceuticals (6, 7). Our approach in designing the ligands prepared in this paper has been biomimetic, as is outlined below.

Enterobactin forms one of the most stable Fe(III) complexes known (8), with an overall stability constant of 10^{49} (9). The backbone of this macrocyclic ligand is derived from three L-serine units, and it utilizes three catechol moieties to sequester Fe(III) in a hexadentate coordination sphere as in Fig. 1a (10–12). However, since the effective ligand is the conjugate base form (the catecholate), the coordination environment of the metal ion is a function of pH. In a series of studies (13–15), Raymond and co-workers have unequivocally established that sequential protonation of the ferric enterobactin complex (three one-proton steps) results in a concomitant shift from a "catechol binding mode" to a "salicylate binding mode" (see Fig. 1). The "arylamides" that possess the structural features depicted in Fig. 1c may thus be considered as "salicylate type"
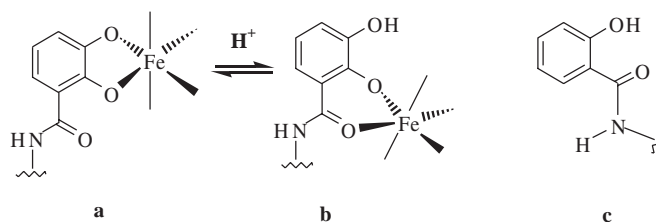
ligands, potentially capable of metal ligation via the phenolate oxygen and the amide carbonyl oxygen.

It was our interest in maltol as an effective bidentate chelating ligand for group 13 metal ions (16, 17) that instigated the investigation of its structural isomer, isomaltol, as yet another naturally occurring bidentate chelator (18). However, once it was established that isomaltol was not a good ligand for the formation of other hexadentate ligands (i.e., its denticity cannot be increased via an imine linkage), due to nucleophilic attack being favored at the C-5 carbon (19), attention was turned to using the amide linkage both as a metal binding group, as well as the "arm" to increase the denticity of the ligand. As a consequence, a bidentate analog Hahm was synthesized starting from the appropriate ethyl ester Hehm (19). In spite of the fact that Al and Ga tris(ligand) complexes could be isolated with Hahm, it was discovered that in H_2O, Hahm undergoes decomposition that is time, concentration, and pH dependent (19).

Given the fact that, in general, the half-life for hydrolysis of an amide bond (in neutral aqueous solution) is ca. 7 years (20), it is clear that replacement of the furan with another aromatic ring system would do much to alleviate the instability of these ligands, not to mention the reduction in the number of steps required for the ligand synthesis. Therefore, we have used derivatives of nicotinic and picolinic acid as (commercially available) starting materials for the formation of new arylamide ligands.
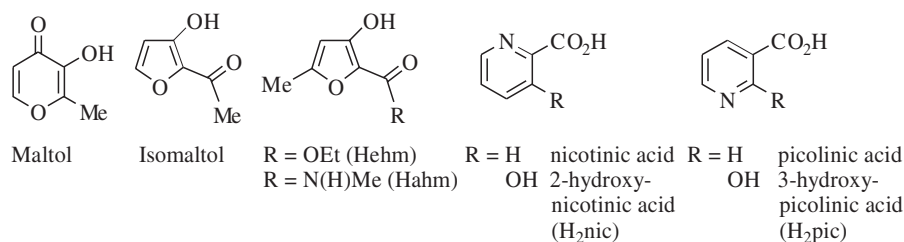
Experimental

Materials and methods

All chemicals were reagent grade and were used as received from commercial vendors (Aldrich and Sigma) unless otherwise stated. 1,1,1-Tris(azidomethyl)ethane was prepared according to a literature procedure (21). THF was distilled from

Na benzophenone ketyl under Ar prior to use; 1,4-dioxane was predried over activated 4Å molecular sieves before use. Water was deionized (Barnstead D8902 and D8904 cartridges) and distilled (Corning MP-1 Megapure still). Plates used for thin-layer chromatography (TLC) were aluminum-supported 0.2 mm silica gel 60 F_{254} (EM Science). Column chromatography was carried out using 230–400 mesh size silica gel

(E. Merck, Silica Gel 60) and the "flash" technique (22), or by using lipophilic Sephadex LH-20™. All reactions were carried out under N_2 unless otherwise noted. The yields reported refer to isolated yields.

Instrumentation

NMR spectra were recorded on Bruker WH-400 (^{1}H NMR, 400 MHz), or Bruker AC-200E (^{1}H NMR, 200 MHz; ^{13}C NMR, 50 MHz) instruments. ^{1}H NMR data are reported as δ downfield from TMS (external reference) at 400 MHz in DMSO-d_6 unless otherwise noted. ^{13}C NMR data are reported as δ downfield from TMS (external reference) at 50 MHz in DMSO-d_6 unless otherwise noted. Infrared (IR) spectra were recorded as KBr disks in the range 4000–400 cm^{-1} on a Perkin Elmer PE 783 spectrophotometer and were referenced to polystyrene unless stated otherwise. Mass spectra (MS) were obtained with a Kratos MS 50 (electron-impact ionization, EI), an AEI MS 9, or a Kratos Concept IIH (fast-atom-bombardment ionization, FAB). Melting points were measured on a Mel-Temp apparatus and are uncorrected. Analyses were performed on a Carlo Erba elemental analyzer by Mr Peter Borda of this department.

Syntheses

Caution! *The handling of polyazides in large quantities may be hazardous. DCC is a severe skin irritant!*

1,1,1-Tris(aminomethyl)ethane (TAME)

TAME was prepared with some modifications to the reported method (21). To a solution of 1,1,1-tris(azidomethyl)ethane (16.8 g, 0.086 mol) in THF (200 mL) at 0°C, lithium aluminium hydride (LAH) (14.0 g, 0.364 mol) was added in small portions over 30 min. The resulting white-grey slurry was stirred at 0°C for 10 min, allowed to warm up to 20°C, and then refluxed for 24 h. The mixture was cooled to 0°C and NaOH (50 mL, 8 M) was added slowly to quench the excess LAH. To the resulting off-white slurry was added Et$_2$O (500 mL) and the reaction mixture was stirred for 30 min. The off-white precipitate was filtered off and washed with Et$_2$O. The combined filtrate and washings were dried (MgSO$_4$), and the solvent was removed on a rotary evaporator to afford TAME (8.6 g, 86%) as a pale yellow oil. ^{1}H NMR and IR spectra of the product thus obtained were identical with those previously reported (21). This product was used without any further purification.

Tris(aminopropyl)amine (TRPN)

TRPN was made by reduction of nitrilotrispropionamide with LAH in THF with some modifications to the reported method (23). The intermediate trisamide was synthesized as follows. To a suspension of acrylamide (43.0 g, 0.60 mol) in H$_2$O (20 mL) was added 26 g of 30% NH$_4$OH (0.22 mol). The solution became clear in ca. 10 min, and the mixture was left stirring at 20°C for 24 h. The precipitate thus formed was filtered, washed with H$_2$O (3 × 10 mL), and dried in vacuo, yielding nitrilotrispropionamide (25 g, 57%). ^{1}H NMR and IR spectra of the product were identical with those previously reported.

To a suspension of the dry trisamide thus obtained (10.0 g, 0.04 mol) in 1000 mL of THF at 0°C, LAH (10.0 g, 0.26 mol) was added in small portions over 30 min. The resulting white-grey slurry was stirred at 0°C for 10 min, allowed to warm up to 20°C, and then stirred for 18 h. The mixture was then cooled to 0°C and NaOH (50 mL, 8 M) was added slowly to quench the excess LAH. To the resulting off-white slurry was added Et$_2$O (500 mL) and the reaction mixture was stirred for 30 min. The off-white precipitate was filtered and washed with Et$_2$O. The organic layer was separated, dried (MgSO$_4$), and evaporated to afford a yellow oil. The crude product was vacuum distilled (0.2 Torr; 1 Torr = 133.3 Pa) to remove the bisamine impurity (ca. 10% by ^{1}H NMR; 65°C) from the product (97–100°C), yielding 2.6 g (35%) of TRPN. ^{1}H and ^{13}C NMR spectra of TRPN thus synthesized were identical with those reported in the literature (23).

Method A: Succinimido 2-hydroxynicotinate (HOSuNic)

To a mixture of 2-hydroxynicotinic acid (1.370 g, 9.85 mmol) in THF (100 mL) was added *N*-hydroxysuccinimide (1.148 g, 9.98 mmol) and DCC (2.275 g, 11.03 mmol). The mixture was then refluxed for 20 h, whereupon it was allowed to cool to 20°C. The white precipitate was filtered, washed with CH$_2$Cl$_2$ (3 × 50 mL), and dried in vacuo. The crude product thus obtained was still contaminated with dicyclohexylurea (DCU). The product was purified via Soxhlet extraction (48 h) using CH$_2$Cl$_2$ to yield 1.02 g (42%) of HOSuNic. ^{1}H NMR: 2.98 (s, 4H^{1,2}), 6.49 (t, 1H$^\beta$, $J = 7$ Hz), 7.99 (dd, 1H$^\gamma$, $J = 7$, 2 Hz), 8.44 (dd, 1H$^\alpha$, $J = 7$, 2 Hz), 12.56 (br s, O*H*). MS (EI), *m/z*: 236 (M$^+$).

HOSuNic   H$_3$NICTREN   HImNic   H$_3$NICTAME
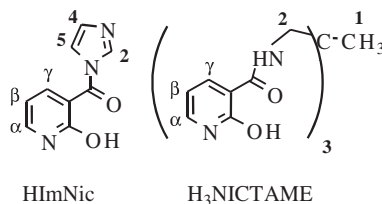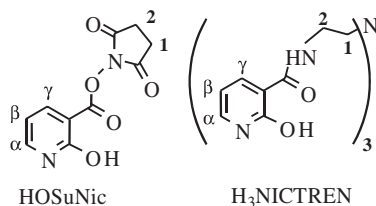
Tris{[((2-hydroxynicotinyl)carbonyl]-2-aminoethyl}amine (H$_3$NICTREN)

To a mixture of HOSuNic (1.17 g, 4.95 mmol) in THF (200 mL) was added TREN (0.240 g, 1.64 mmol) in one portion. The resultant mixture was refluxed for 18 h, whereupon it was left to cool to 20°C. The white precipitate was filtered, washed

with CH$_2$Cl$_2$ and Et$_2$O, and dried in vacuo to afford H$_3$NIC-TREN (0.73 g, 87%), mp 242°C (dec.). IR: 3640–2600 (br, ν$_{OH}$), 3280 (m, ν$_{NH}$), 1680 (s, ν$_{C=O}$), 1610 (m, ν$_{C=C}$), 1560 (s, amide II (24)), 1473 (m, ν$_{C=C}$), 1328, 1255, 1060, 980. ^{1}H NMR: 2.68 (t, 6H^1, $J = 6$ Hz), 3.10–3.60 (partially obscured m, 6H^2), 6.43 (t, 3H$^\beta$, $J = 6$ Hz), 7.64 (dd, 3H$^\gamma$, $J = 6$, 4 Hz), 8.28

(dd, 3H$^\alpha$, J = 6, 4 Hz), 9.79 (t, 3H, C(O)NH, J = 6 Hz), 12.20 (br s, 3H, OH). ^{13}C NMR (DMSO-d_6): 37.42 (C1), 53.46 (C2), 106.14 (Cb), 120.63 (Cγ), 139.30 (Cα), 143.77 (Cδ), 162.32 (*C*-OH), 163.36 (*C*=O). Anal. calcd. (found) for C$_{24}$H$_{27}$N$_7$O$_6$·0.5H$_2$O: C 55.60 (55.42), H 5.21 (5.33), N 18.90 (18.83).

Method B: N-*(2-Hydroxynicotinyl)-imidazole (HImNic)*
To a mixture of 2-hydroxynicotinic acid (5.34 g, 38.4 mmol) in THF (200 mL) was added CDI (6.43 g, 39.4 mmol) in one portion. The mixture was refluxed for 19 h. After cooling the reaction mixture to 20°C, the white precipitate was filtered, washed with Et$_2$O, and dried in vacuo to afford HImNic (6.65 g, 98%). ^{1}H NMR: 6.38 (t, 1H$^\beta$, J = 6.6 Hz), 7.05 (dd, 1H^4, J = 1.6, 0.8 Hz), 7.61 (t, 1H^5, J = 1.6 Hz), 7.74 (dd, 1H$^\gamma$, J = 6.3, 2.2 Hz), 7.93 (dd, 1H$^\alpha$, J = 6.3, 2.2 Hz), 8.16 (t, 1H^2, J = 0.8 Hz), 12.32 (br s, OH). MS (EI), *m/z*: 189 (M$^+$). Anal. calcd. (found) for C$_9$H$_7$N$_3$O$_2$: C 57.14 (56.95), H 3.73 (3.81), N 22.21 (22.15).

Tris{[(2-hydroxynicotinyl)carbonyl]-2-aminoethyl}amine (H$_3$NICTREN)
To a mixture of HImNic (6.30 g, 33.3 mmol) in 1,4-dioxan (400 mL) was added TREN (1.56 g, 10.67 mmol) in one portion. The resulting mixture was refluxed for 18 h. After cooling the reaction mixture to 20°C, the precipitate was filtered, washed with THF and Et$_2$O, and dried in vacuo to afford H$_3$NICTREN as a white solid (5.20 g, 95%). ^{1}H NMR, ^{13}C NMR, IR, and MS spectra were identical to those reported for the sample obtained by Method A. Anal. calcd. (found) for C$_{24}$H$_{27}$N$_7$O$_6$·0.25H$_2$O: C 56.08 (56.15), H 5.39 (5.57), N 19.07 (19.07).

1,1,1-Tris{[(2-hydroxynicotinyl)carbonyl]-2-aminomethyl}ethane (H$_3$NICTAME)
To a mixture of HImNic (6.05 g, 32.0 mmol) in 1,4-dioxan (400 mL) was added TAME (1.10 g, 9.39 mmol) in one portion. The resulting mixture was refluxed for 19 h. After cooling the reaction mixture to 20°C, the precipitate was filtered, washed with THF and Et$_2$O, and dried in vacuo to afford H$_3$NICTAME as an off-white solid (4.22 g, 89 %), mp 270°C (dec.). IR: 3600–2600 (br, ν_{OH}), 3280 (m, ν_{NH}), 1665 (s, $\nu_{C=O}$), 1600 (m, $\nu_{C=C}$), 1562 (s, amide II), 1480 (m, $\nu_{C=C}$), 1430, 1320, 1235, 1150, 790, 770. ^{1}H NMR: 0.91 (s, 3H^I), 3.14–3.47 (partially obscured d, 6H^2, J = 6 Hz), 6.46 (t, 3H$^\beta$ J = 6 Hz), 7.69 (dd, 3H$^\gamma$, J = 8, 1.2 Hz), 8.30 (dd, 3H$^\alpha$, J = 8, 1.2 Hz), 10.01 (t, 3H, C(O)NH, J = 6 Hz), 12.38 (br s, 3H, OH). MS (FAB), *m/z*: 481 (M+H)$^+$. Anal. calcd. (found) for C$_{23}$H$_{24}$N$_6$O$_6$·H$_2$O: C 55.42 (55.68), H 5.22 (5.28), N 16.87 (16.55).

N^1,N^5,N^{10}-*Tris(2-hydroxynicotinyl)spermidine (H$_3$NICSPERM)*
To a suspension of HImNic (2.639 g, 13.96 mmol) in 1,4-dioxane (200 mL) was added spermidine (0.658 g, 4.53 mmol) in one portion. The resulting mixture was refluxed for 19 h. After cooling the reaction mixture to 20°C, the brown-orange precipitate was filtered, washed with Et$_2$O, and dried in vacuo to yield 1.611 g of the crude product; 205 mg of this was column chromatographed on lipophilic Sephadex LH-20™ (3 × 120 cm column; eluant: 50% MeOH in EtOAc) to afford pure

product (150 mg, 73% recovery), equivalent to a 51% overall yield; mp 115–117°C. TLC (eluant: 50% MeOH in EtOAc) R$_f$ = 0.3. IR: 3600–2600 (br,ν_{OH}), 3260 (m, ν_{NH}), 1675 (s, $\nu_{C=O}$), 1605 (m, $\nu_{C=C}$), 1560 (s, amide II), 1230, 775. ^{1}H NMR (δ at 200 MHz in DMSO-d_6): 1.3–1.9 (three overlapping m, 6 H^{3,7,8}), 2.9–3.6 (partially obscured overlapping m, 8H^{2,4,6,9}), 6.03–6.22 (m, 1H$^\beta$), 6.40–6.51 (m, 2H$^{\beta',\beta''}$), 7.24–7.45 (two overlapping m, 2H$^{\alpha,\gamma}$), 7.60–7.75 (m, 2H$^{\gamma',\gamma''}$), 8.22–8.38 (m, 2H$^{\alpha',\alpha''}$), 9.60–9.90 (m, 2H, C(O)NH), 11.85 (br s, 1H, OH), 12.45 (br s, 2H, OH). MS (FAB), *m/z*: 510 ± 1 (M+H)$^+$. Anal. calcd. (found) for C$_{25}$H$_{28}$N$_6$O$_6$·H$_2$O: C 57.03 (57.13), H 5.74 (5.80), N 15.96 (15.82).

H$_3$NICSPERM
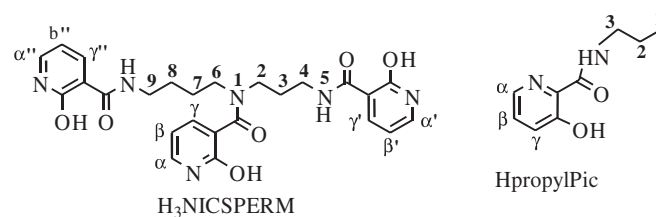
HpropylPic

[(3-Hydroxypicolinyl)carbonyl]propylamine (HpropylPic)
To a mixture of 3-hydroxypicolinic acid (1.48 g, 10.6 mmol) in THF (200 mL) was added CDI (1.92 g, 11.8 mmol) in one portion. The mixture was refluxed for 2 h whereupon *n*-propylamine (10.1 g, 0.12 mol) was added and the resultant mixture was refluxed for a further 19 h. After cooling the reaction mixture to 20°C, the volatiles were removed under reduced pressure and the resultant oil was column chromatographed on silica gel (eluant: 50% pentane in Et$_2$O, R$_f$ = 0.84) to afford Hpropylpic (1.40 g, 74%) as a yellow-brown liquid. IR (neat on KBr plates): 3600–2600 (br, ν_{OH}), 3380 (m, ν_{N-H}), 1650 (s, $\nu_{C=O}$), 1580 (m, $\nu_{C=C}$), 1535 (s, amide II), 1450 (m, $\nu_{C=C}$), 1340, 1295, 1255, 1195, 810, 795. ^{1}H NMR: 0.85 (t, 3H^I, J = 7 Hz), 1.54 (m, 2H^2), 3.25 (dt, 2H^3, J = 8, 7 Hz), 7.36 (dd, 1H$^\gamma$, J = 8, 0.8 Hz), 7.48 (dd, 1H$^\beta$, J = 8, 4 Hz), 8.12 (dd, 1H$^\alpha$, J = 4, 0.8 Hz), 9.14 (t, 1H, C(O)NH, J = 6 Hz), 12.70 (br s, OH). ^{13}C NMR: 11.32 (C1), 22.27 (C2), 40.05 (C3), 125.84 (Cγ), 128.95 (Cβ), 131.49 (Cα), 139.66 (*C*C(O)NH), 157.37 (*C*-OH), 168.70 (*C*=O). Exact Mass calcd. (found) for C$_9$H$_{12}$N$_2$O$_2$: 180.0904 (180.0898). Anal. calcd. (found) for C$_9$H$_{12}$N$_2$O$_2$: C 59.99 (59.77), H 6.71 (6.78), N 15.55 (15.50).

1,1,1-Tris{[(3-hydroxypicolinyl)carbonyl]-2-aminomethyl}-ethane (H$_3$PICTAME)
To a mixture of 3-hydroxypicolinic acid (5.34 g, 38.39 mmol) in THF (150 mL) was added CDI (6.43 g, 39.65 mmol) in one portion. The mixture was refluxed for 5 h whereupon TAME (1.50 g, 12.80 mmol) was added and the solution was refluxed for a further 26 h. After cooling the reaction mixture to 20°C, the precipitate was filtered and the filtrate was concentrated in vacuo to yield a dark reddish-brown residue. This residue was redissolved in a minimum amount of hot MeOH (ca. 40 mL), which, after cooling to room temperature, was triturated with Et$_2$O to yield the product as a brown solid (1.25 g, 20%), mp 165–167°C. X-ray quality crystals were obtained by slow evaporation of a MeOH:Et$_2$O (1:20) solution at room temperature (rt). IR: 3600–2600 (br, ν_{OH}), 3355 (m, ν_{NH}), 1650 (s, $\nu_{C=O}$), 1580 (m, $\nu_{C=C}$), 1530 (s, amide II), 1448 (m, $\nu_{C=C}$), 1355, 1315, 1295, 1245, 1200, 1160, 810, 695, 660. ^{1}H NMR:

0.88 (s, 3H^I), 3.20–3.41 (partially obscured d, 6H^2, J = 6 Hz), 7.43 (dd, 3H$^\gamma$, J = 8, 0.8 Hz), 7.55 (dd, 3H$^\beta$, J = 8, 4 Hz), 8.19 (dd, 3H$^\alpha$, J = 4, 0.8 Hz), 9.62 (t, 3H, C(O)NH, J = 6 Hz), 12.46

(br s, 3H, OH). MS (FAB), m/z: 481 (M+H)$^+$. Anal. calcd. (found) for $C_{23}H_{24}N_6O_6$: C 57.50 (57.39), H 5.03 (4.90), N 17.49 (17.55).

H$_3$PICTAME   H$_3$PICTREN   PICTREN   PICTAME
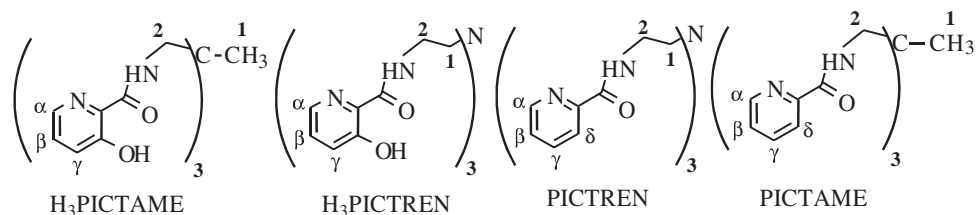
Tris{[(3-hydroxypicolinyl)carbonyl]-2-aminoethyl}amine (H$_3$PICTREN)

To a mixture of 3-hydroxypicolinic acid (2.52 g, 18.12 mmol) in THF (150 mL) was added CDI (3.50 g, 21.6 mmol) in one portion. The mixture was refluxed for 5 h whereupon TREN (0.883 g, 6.04 mmol) was added and the solution was refluxed for a further 18 h. After cooling the reaction mixture to 20°C, the precipitate was filtered and the filtrate was concentrated in vacuo to yield a dark reddish-brown residue. This residue was redissolved in a minimum amount of hot MeOH (ca. 20 mL), which, after cooling to rt, was triturated with Et$_2$O to yield the product as a light-brown solid (2.15 g, 70%), mp 156–158°C. IR: 3600–2700 (br, ν_{OH}), 3350 (m, ν_{NH}), 1640 (s, $\nu_{C=O}$), 1590 (m, $\nu_{C=C}$), 1540 (s, amide II), 1450 (m, $\nu_{C=C}$), 1300, 1240, 1200, 1180, 1150, 860, 820, 685, 665. ^{1}H NMR: 2.78 (t, 6H^I, J = 6 Hz), 3.36–3.47 (partially obscured m, 6H^2), 7.33 (dd, 3H$^\gamma$, J = 8, 0.8 Hz), 7.42 (dd, 3H$^\beta$, J = 8, 4 Hz), 7.97 (dd, 3H$^\alpha$, J = 4, 0.8 Hz), 8.96 (t, 3H, C(O)NH, J = 6 Hz), 12.52 (br s, 3H, OH). MS (FAB), m/z: 510 (M+H)$^+$. Anal. calcd. (found) for $C_{24}H_{27}N_7O_6$: C 56.58 (56.46), H 5.34 (5.41), N 19.24 (19.21).

Tris{[(picolinyl)carbonyl]-2-aminoethyl}amine (PICTREN)

To a mixture of picolinic acid (3.0 g, 24.4 mmol) in THF (200 mL) was added CDI (4.35 g, 26.8 mmol) in one portion. The resultant mixture was refluxed for 1 h whereupon TREN (1.17 g, 8.02 mmol) was added and the mixture was refluxed for a further 19 h. After cooling the reaction mixture to 20°C and removal of the solvent under reduced pressure, the dark-brown residue thus obtained was column chromatographed on lipophilic Sephadex LH-20™ (3 × 120 cm column; eluant: MeOH) to afford PICTREN (3.43 g, 93%) as a deep red-brown viscous liquid. IR (in CHCl$_3$): 3390 (m, ν_{NH}), 1665 (s, $\nu_{C=O}$). ^{1}H NMR: 2.76 (t, 6H^I, J = 6 Hz), 3.34–3.50 (partially obscured m, 6H^2), 7.49-7.56 (m, 3Hβ), 7.90–8.00 (m, 6H$^{\gamma,\delta}$), 8.43-8.47 (m, 3H$^\alpha$), 8.70 (t, 3H, C(O)NH, J = 6 Hz). MS (FAB), m/z: 462 (M+H)$^+$. Anal. calcd. (found) for $C_{24}H_{27}N_7O_3\cdot0.5H_2O$: C 61.26 (60.99), H 6.00 (5.94), N 20.84 (20.92).

1,1,1-Tris{[(picolinyl)carbonyl]-2-aminomethyl}ethane (PICTAME)

To a mixture of picolinic acid (1.576 g, 12.80 mmol) in THF (150 mL) was added CDI (2.283 g, 14.08 mmol) in one portion. The resultant mixture was refluxed for 2 h whereupon TAME (0.5 g, 4.30 mmol) was added and the mixture was

refluxed for a further 19 h. After cooling the reaction mixture to 20°C, and removal of the solvent under reduced pressure, the residue so obtained was column chromatographed on silica gel (eluant: 5% MeOH:45% Et$_2$O:50% EtOAc; R_f = 0.58) to afford PICTAME (1.30 g, 70%) as a white solid, mp 207–208°C. IR: 1670 (s, $\nu_{C=O}$), 1590 (m, $\nu_{C=C}$), 1535 (s, amide II), 1465 (m, $\nu_{C=C}$), 1435, 1335, 1000, 760, 690. ^{1}H NMR: 0.53 (s, 3H^I), 3.22 (d, 6H^2, J = 6 Hz), 7.62 (ddd, 3H$^\beta$, J = 8, 4, 1.2 Hz), 8.01 (dt, 3H$^\gamma$, J = 8, 8, 1.6 Hz), 8.06-8.16 (m, 3H$^\delta$), 8.66-8.74 (m, 3H$^\alpha$), 9.37 (t, 3H, C(O)NH, J = 6 Hz). MS (FAB), m/z: 433 (M+H)$^+$. Anal. calcd. (found) for $C_{23}H_{24}N_6O_3$: C 63.88 (63.63), H 5.59 (5.53), N 19.43 (19.20).

H$_3$PICSPERM   H$_3$PICTRPN
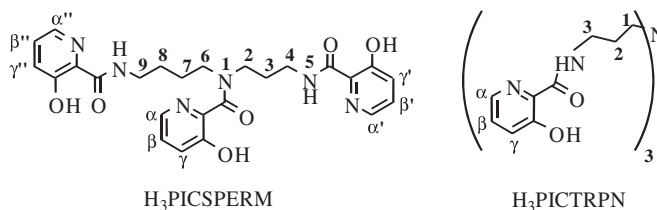
N^1,N^5,N^{10}-Tris(3-hydroxypicolinyl)spermidine (H$_3$PICSPERM)

To a mixture of 3-hydroxypicolinic acid (2.657 g, 19.1 mmol) in THF (275 mL), CDI (3.103 g, 19.1 mmol) was added and the solution refluxed for 3 h. Spermidine (0.87 g, 5.97 mmol) was added to the mixture, which was refluxed for an additional 15 h. After cooling the reaction mixture to 20°C, the solution was filtered and the filtrate was concentrated in vacuo to a yellowish oil. The slow-moving contaminants (R_f 0.05) in the mixture were removed by column chromatography on silica gel (eluant: 5% MeOH in EtOAc). Combining the appropriate fractions and evaporating the solvent yielded a yellow oil. This material was then triturated with MeOH (ca. 50 mL) to afford H$_3$PICSPERM (1.31 g, 42%) as a white solid, mp 99–100°C. TLC (eluant: 5% MeOH in EtOAc) R_f = 0.48. IR: 3600–2600 (br, ν_{OH}), 3360 (m, ν_{NH}), 1650 (s, $\nu_{C=O}$), 1610 (m, $\nu_{C=C}$), 1535 (s, amide II), 1445 (m, $\nu_{C=C}$), 1610, 1390, 1190, 990, 810, 795. ^{1}H NMR (δ at 400 MHz in CDCl$_3$): 1.62–2.13 (series of overlapping m, 6H^{3,7,8}), 3.43–3.60 (m, 5H$^{4,6',9}$), 3.64, 4.04, 4.12 (three t each, 3H$^{2,6''}$, J = 6 Hz), 7.20–7.37 (m, 6H$^{\beta,\beta',\beta'',\gamma,\gamma,\gamma'}$), 7.98–8.24 (m, 3H$^{\alpha,\alpha',\alpha''}$), 8.33, 8.56 (two br s, 2H, C(O)NH, $W_{1/2}$ = 14 Hz), 12.2 (br s, 2H, OH), 12.3 (br s, 1H, OH). ^{13}C NMR (δ at 50 MHz in CDCl$_3$): 169.4, 169.1, 168.9, 158.8, 158.7, 157.8, 139.4, 138.8, 134.3, 131.4, 128.6,

127.4, 126.1, 102.9, 49.7, 47.8, 38.8, 36.3, 28.8, 27.6, 26.7, 24.6. MS (FAB), m/z: 509 (M+H)$^+$. Anal. calcd. (found) for $C_{25}H_{28}N_6O_6$: C 59.05 (59.06), H 5.55 (5.63), N 16.53 (16.60).

Tris{[(3-hydroxypicolinyl)carbonyl]-2-aminopropyl}amine (H₃PICTRPN)

Tris{[(3-hydroxypicolinyl)carbonyl]-2-aminopropyl}amine (H$_3$PICTRPN)

To a mixture of 3-hydroxypicolinic acid (1.145 g, 8.23 mmol) in THF (120 mL) was added CDI (1.335 g, 8.23 mmol) in one portion. The mixture was refluxed for 2 h whereupon TRPN (0.5 g, 2.66 mmol) was added and the resultant mixture was refluxed for a further 19 h. After cooling the reddish-brown reaction mixture to 20°C, the solvent was removed under reduced pressure and the viscous dark-brown liquid was redissolved in a minimum amount of hot MeOH (ca.40 mL) and triturated with Et$_2$O to remove any unreacted starting acid (0.45 g, 39%) that precipitated. The filtrate was concentrated under reduced pressure and the brownish oil thus obtained was column chromatographed twice on lipophilic Sephadex LH-20™ (3 × 120 cm column; eluant: MeOH) and on silica gel (eluant: 10% MeOH in EtOAc, R_f = 0.13) to afford H$_3$PICTRPN (0.13 g, 9%) as a glassy (sticky) brown solid. IR: 3600–2600 (br, ν_{OH}), 3350 (m, ν_{NH}), 1655 (s, $\nu_{C=O}$), 1595 (m, $\nu_{C=C}$), 1540 (s, amide II), 1445 (m, $\nu_{C=C}$), 1350, 1289, 1248, 1198, 1150, 807, 695. ^{1}H NMR: 1.75 (t, 6H^1, J = 6 Hz), 2.35–2.70 (partially obscured m, 6H^2), 3.35 (dt, 6H^3, J = 8, 7 Hz), 7.38 (d, 3H$^\gamma$, J = 8 Hz), 7.48 (dd, 3H$^\beta$, J = 8, 3 Hz), 8.10 (d, 3H$^\alpha$, J = 3 Hz), 9.22 (br s, 3H, C(O)NH, $W_{1/2}$ = 20 Hz), 12.62 (br s, 3H, OH). MS (FAB), m/z: 552 (M+H)$^+$. Anal. calcd. (found) for $C_{27}H_{33}N_7O_6 \cdot 0.25H_2O$: C 58.32 (58.43), H 6.07 (5.90), N 17.63 (17.55).

Potentiometric equilibrium measurements

All potentiometric measurements on H$_3$NICTREN and H$_3$NICTAME were made with an automatic titrator system consisting of a Fisher model 950 digital pH meter equipped with Orion–Ross glass and calomel reference electrodes, a Metrohm Dosimat model 665 autoburet, and water-jacketed titration vessels maintained at 25.0 ± 0.1°C with a Julabo UC circulating bath (25). Both autoburet and pH meter were interfaced to an IBM-compatible PC so that the titrations were automated. During the titrations, the solutions were kept under an argon atmosphere that was first passed through 2 M NaOH solution.

The electrodes were calibrated before each titration, and often afterwards, by titrating a known amount of aqueous HCl with a known concentration of NaOH. A plot of mV (calculated) vs. pH gave a working slope and intercept so that the pH could be read directly as –log[H$^+$]. The value of pK_w used was 13.76.

All solutions were prepared at an ionic strength of 0.16 M NaCl. Carbonate-free NaOH (~0.16 M) was prepared with deionized, distilled water that was boiled and purged with argon while cooling to ensure removal of CO$_2$. This solution was standardized potentiometrically with potassium hydrogen phthalate. Standard HCl solutions were prepared similarly and were standardized with the NaOH prepared above. Stock ligand solutions (~ 0.5 mM) were prepared using deionized, distilled water and were used within 3–4 days. The compounds were titrated in the pH range 2–11.5; a minimum of five titrations was performed for each compound.

Potentiometric calculations

The deprotonation constants of the ligands were calculated using the program BEST (26). The program sets up simultaneous mass-balance equations for all the components present at each addition of base and calculates the pH at each data point according to the current set of stability constants and total concentrations of each component. The stability constants are iteratively varied to minimize the sum of the square of the difference between observed (pH$_{obs}$) and calculated (pH$_{calc}$) pH values. An indication of the fit is given by σ_{fit}, where σ_{fit} is

$$\sigma_{fit} = \Sigma\,(pH_{calc} - pH_{obs})^2/(N-1)$$

and N is the total number of data points (typically ~100). In all the titrations considered, $\sigma_{fit} < 0.01$. The final calculated deprotonation constants are the average of the deprotonation constants determined from individual titrations; an estimate of the error in these values is given by one standard deviation (1σ) for these results.

X-ray crystallographic analysis of H₃PICTAME

X-ray crystallographic analysis of H$_3$PICTAME

Crystallographic data for H$_3$PICTAME appear in Table 1. The final unit-cell parameters were obtained by least squares on the setting angles for 25 reflections with 2θ = 55.1°–82.4°. The intensities of three standard reflections, measured every 200 reflections throughout the data collection, showed only small random fluctuations. The data were processed,[2] corrected for Lorentz and polarization effects, and for absorption (empirical, based on azimuthal scans).

The structure was solved by direct methods. Non-hydrogen atoms were refined with anisotropic thermal parameters, the O-bound hydrogen atoms were refined with isotropic thermal parameters, and the remaining hydrogen atoms were fixed in calculated positions with N—H = 0.91 Å, C—H = 0.98 Å, and $B_H = 1.2\,B_{bonded\ atom}$. A correction for secondary extinction was applied (Zachariasen type, isotropic), the final value of the extinction coefficient being 5.7(3) × 10^{-7}. Neutral atom scattering factors for all atoms and anomalous dispersion corrections for the non-hydrogen atoms were taken from the *International tables for X-ray crystallography* (27). Final atomic coordinates and equivalent isotropic thermal parameters, bond lengths, bond angles, and hydrogen bond geometry appear in Tables 2–5, respectively. Hydrogen atom parameters, anisotropic thermal parameters, torsion angles, intermolecular contacts, and least-squares planes are available as supplementary material.[3]

Results and discussion

Synthetic procedures

HOSu/DCC method (Method A) (28)

Depending on the nature of the starting materials, *N,N′*-dicyclohexylcarbodiimide (DCC) by itself can act in situ as a

---

2 *teXan*: Crystal Structure Analysis Package. Molecular Structure Corp., The Woodlands, Texas. 1985 and 1992.

3 Supplementary material mentioned in the text can be purchased from: The Depository of Unpublished Data, Document Delivery, CISTI, National Research Council Canada, Ottawa, Canada K1A 0S2. Tables of hydrogen atom coordinates and bond distances have also been deposited with the Cambridge Crystallographic Data Centre, and can be obtained on request from The Director, Cambridge Crystallographic Centre, 12 Union Road, Cambridge, CB1 1EZ. U.K.

Table 1. Crystallographic data for H₃PICTAME.[a]

Formula	$C_{23}H_{24}N_6O_6$
fw	480.48
Crystal system	Monoclinic
Space group	$P2_1/a$
a, Å	10.257(2)
b, Å	15.572(3)
c, Å	15.208(2)
β,°	96.124(15)
V, Å³	2415.2(8)
Z	4
ρ_{calc}, g/cm³	1.321
$F(000)$	1008
Radiation (λ, Å)	Cu (1.54178)
μ, cm⁻¹	8.21
Crystal size, mm	$0.12 \times 0.25 \times 0.30$
Transmission factors	0.97–1.00
Scan type	ω–2θ
Scan range, deg in ω	$0.89 + 0.20 \tan\theta$
Scan speed, deg/min	32 (up to 8 rescans)
Data collected	$+h, +k, \pm l$
$2\theta_{max}$, deg	155
Crystal decay, %	Negligible
Total reflections	5368
Total unique reflections	5099
R_{merge}	0.022
Reflections with $I \geq 3\sigma(I)$	2506
No. of variables	329
R	0.041
R_w	0.038
gof	2.27
Max Δ/σ (final cycle)	0.0003
Residual density e/Å³	–0.12 to 0.25

[a] Temperature 294 K, Rigaku AFC6S diffractometer, graphite monochromator, takeoff angle 6.0°, aperture 6.0 × 6.0 mm at a distance of 285 mm from the crystal, stationary background counts at each end of the scan (scan/background time ratio 2:1), $\sigma^2(F^2) = [S^2(C + 4B)]/Lp^2$ (S = scan rate, C = scan count, B = normalized background count), function minimized $\Sigma w(|F_o| - |F_c|)^2$ where $w = 4F_o/\sigma^2(F_o^2)$, $R = \Sigma ||F_o| - |F_c||/\Sigma |F_o|$, $Rw = (\Sigma w(|F_o| - |F_c|)^2/\Sigma w|F_o|^2)^{1/2}$, and gof $= [\Sigma w(|F_o| - |F_c|)^2/(m - n)]^{1/2}$. Values given for R, R_w, and gof are based on those reflections with $I \geq 3\sigma(I)$.

Table 2. Final atomic coordinates (fractional) and B_{eq} (Å²) for H₃PICTAME.[a]

Atom	x	y	z	B_{eq}
O(1)	0.5379(2)	0.19534(12)	0.22904(12)	5.56(5)
O(2)	0.5327(3)	0.0389(2)	0.1759(2)	7.88(8)
O(3)	0.3223(2)	0.57156(12)	0.45428(12)	5.52(5)
O(4)	0.1540(2)	0.69186(15)	0.46730(15)	6.83(7)
O(5)	0.4835(2)	0.51490(15)	0.14869(13)	6.53(6)
O(6)	0.6443(4)	0.5781(2)	0.0469(2)	9.72(9)
N(1)	0.4708(2)	0.22750(13)	0.36175(14)	4.62(6)
N(2)	0.3842(3)	0.0661(2)	0.3798(2)	6.38(8)
N(3)	0.3942(2)	0.54131(13)	0.32155(14)	4.60(6)
N(4)	0.2565(3)	0.67422(15)	0.24658(15)	5.64(7)
N(5)	0.4902(2)	0.37287(15)	0.18000(14)	5.10(6)
N(6)	0.6955(3)	0.3500(2)	0.0871(2)	8.09(10)
C(1)	0.4177(3)	0.3826(2)	0.3313(2)	3.88(6)
C(2)	0.2945(3)	0.3734(2)	0.3794(2)	5.10(7)
C(3)	0.5197(3)	0.3153(2)	0.3664(2)	4.18(6)
C(4)	0.4863(3)	0.1737(2)	0.2961(2)	4.52(7)
C(5)	0.4439(3)	0.0838(2)	0.3080(2)	4.87(8)
C(6)	0.4710(3)	0.0208(2)	0.2472(2)	5.76(9)
C(7)	0.4358(4)	–0.0632(2)	0.2641(3)	7.41(11)
C(8)	0.3773(4)	–0.0809(2)	0.3373(3)	8.10(12)
C(9)	0.3524(4)	–0.0152(2)	0.3938(3)	8.06(12)
C(10)	0.4804(3)	0.4707(2)	0.3516(2)	4.30(6)
C(11)	0.3232(3)	0.5867(2)	0.3741(2)	4.49(7)
C(12)	0.2444(3)	0.6585(2)	0.3317(2)	4.49(7)
C(13)	0.1655(3)	0.7071(2)	0.3813(2)	5.04(8)
C(14)	0.0950(3)	0.7739(2)	0.3397(2)	6.52(10)
C(15)	0.1050(4)	0.7895(2)	0.2529(3)	7.03(10)
C(16)	0.1874(4)	0.7392(2)	0.2085(2)	6.81(10)
C(17)	0.3797(3)	0.3717(2)	0.2318(2)	4.63(7)
C(18)	0.5335(3)	0.4421(2)	0.1416(2)	5.60(9)
C(19)	0.6459(4)	0.4294(3)	0.0898(2)	6.42(10)
C(20)	0.6950(4)	0.4972(3)	0.0444(2)	8.12(13)
C(21)	0.7968(5)	0.4827(4)	–0.0053(3)	10.5(2)
C(22)	0.8473(5)	0.4034(5)	–0.0085(3)	11.9(2)
C(23)	0.7953(5)	0.3367(4)	0.0397(3)	10.36(15)

[a] $B_{eq} = (8/3)\pi^2 \Sigma\Sigma(U_{ij} a_i^* a_j^* (\mathbf{a}_i \cdot \mathbf{a}_j))$.

dehydrative coupling reagent, leading to the formation of the amide bond. In the present work, however, it was important that an activated ester be isolated, as the reaction between the amines (e.g., TREN or TAME) and the pyridine carboxylic acids used was fast enough to result in the quantitative precipitation of the corresponding ammonium salt. The main drawback in using this method was the practical difficulty of purifying the activated ester from the dicyclohexylurea that formed as a side product. This problem was circumvented by adopting the more efficient CDI method.

CDI method (Method B) (31)
The advantage of method B is that it obviates the intermediacy of DCC (and hence the DCU side product). The side products formed in method B (imidazole and CO_2) are easier to remove. This method, although it involves two steps, allows for a single-step synthesis of the amide unless practical reasons call for

the isolation of the intermediate imidazolide. Due to the lack of sufficient solubility in THF (bp 67°C), the *N*-acylimidazolide of 2-hydroxynicotinic acid was isolated, and the next step performed in a more suitable, i.e., more polar, solvent, dioxane. Conveniently enough, these crystalline intermediates, although highly reactive in solution towards nucleophiles such as amine nitrogen, are stable in air at room temperature for at least a week.

X-ray crystal structure of H₃PICTAME
In X-ray crystallography, the main criterion for identification of an H-bond is the distance between the hydrogen and the acceptor atom (that is, the distance H⋯A in B—H⋯A where A and B are frequently nitrogen or oxygen atoms). However, in using X-ray diffraction data to extract bond distances involving a hydrogen atom, one must be aware of the fact that such bond lengths are systematically shortened (relative to the "true" internuclear separation) since these distances are, strictly speaking, a measure of the distance between the

Table 3. Bond lengths (Å) in H$_3$PICTAME with estimated standard deviations in parentheses.

Bond	Length	Bond	Length
O(1)—C(4)	1.245(3)	O(2)—C(6)	1.343(4)
O(3)—C(11)	1.243(3)	O(4)—C(13)	1.347(3)
O(5)—C(18)	1.254(3)	O(6)—C(20)	1.365(5)
N(1)—C(3)	1.456(3)	N(1)—C(4)	1.326(3)
N(2)—C(5)	1.336(3)	N(2)—C(9)	1.331(4)
N(3)—C(10)	1.454(3)	N(3)—C(11)	1.339(3)
N(4)—C(12)	1.336(3)	N(4)—C(16)	1.332(4)
N(5)—C(17)	1.447(3)	N(5)—C(18)	1.325(4)
N(6)—C(19)	1.339(4)	N(6)—C(23)	1.330(5)
C(1)—C(2)	1.532(3)	C(1)—C(3)	1.535(3)
C(1)—C(10)	1.533(3)	C(1)—C(17)	1.531(3)
C(4)—C(5)	1.482(4)	C(5)—C(6)	1.396(4)
C(6)—C(7)	1.388(4)	C(7)—C(8)	1.349(5)
C(8)—C(9)	1.377(5)	C(11)—C(12)	1.486(4)
C(12)—C(13)	1.388(4)	C(13)—C(14)	1.381(4)
C(14)—C(15)	1.357(4)	C(15)—C(16)	1.381(4)
C(18)—C(19)	1.478(4)	C(19)—C(20)	1.385(5)
C(20)—C(21)	1.370(6)	C(21)—C(22)	1.342(7)
C(22)—C(23)	1.409(7)		

Table 4. Bond angles (deg) in H$_3$PICTAME with estimated standard deviations in parentheses.

Bonds	Angle (deg)	Bonds	Angle (deg)
C(3)-N(1)-C(4)	124.2(2)	C(5)-N(2)-C(9)	117.9(3)
C(10)-N(3)-C(11)	124.2(2)	C(12)-N(4)-C(16)	117.4(3)
C(17)-N(5)-C(18)	124.7(3)	C(19)-N(6)-C(23)	118.5(4)
C(2)-C(1)-C(3)	109.7(2)	C(2)-C(1)-C(10)	109.7(2)
C(2)-C(1)-C(17)	109.0(2)	C(3)-C(1)-C(10)	106.5(2)
C(3)-C(1)-C(17)	111.1(2)	C(10)-C(1)-C(17)	110.8(2)
N(1)-C(3)-C(1)	113.9(2)	O(1)-C(4)-N(1)	122.7(3)
O(1)-C(4)-C(5)	120.8(3)	N(1)-C(4)-C(5)	116.4(3)
N(2)-C(5)-C(4)	117.4(3)	N(2)-C(5)-C(6)	122.5(3)
C(4)-C(5)-C(6)	120.1(3)	O(2)-C(6)-C(5)	122.1(3)
O(2)-C(6)-C(7)	120.1(3)	C(5)-C(6)-C(7)	117.8(3)
C(6)-C(7)-C(8)	119.5(3)	C(7)-C(8)-C(9)	119.5(3)
N(2)-C(9)-C(8)	122.8(3)	N(3)-C(10)-C(1)	112.7(2)
O(3)-C(11)-N(3)	123.2(3)	O(3)-C(11)-C(12)	120.5(3)
N(3)—C(11)-C(12)	116.3(3)	N(4)-C(12)-C(11)	117.1(3)
N(4)-C(12)-C(13)	123.1(3)	C(11)-C(12)-C(13)	119.7(3)
O(4)-C(13)-C(12)	123.2(3)	O(4)-C(13)-C(14)	118.8(3)
C(12)-C(13)-C(14)	117.9(3)	C(13)-C(14)-C(15)	119.4(3)
C(14)-C(15)-C(16)	119.2(3)	N(4)-C(16)-C(15)	122.9(3)
N(5)-C(17)-C(1)	113.9(2)	O(5)-C(18)-N(5)	122.6(3)
O(5)-C(18)-C(19)	121.1(3)	N(5)-C(18)-C(19)	116.4(3)
N(6)-C(19)-C(18)	117.4(3)	N(6)-C(19)-C(20)	121.9(4)
C(18)-C(19)-C(20)	120.7(4)	O(6)-C(20)-C(19)	121.9(4)
O(6)-C(20)-C(21)	118.8(5)	C(19)-C(20)-C(21)	119.3(5)
C(20)-C(21)-C(22)	119.4(6)	C(21)-C(22)-C(23)	119.3(5)
N(6)-C(23)-C(22)	121.5(5)		

centroids of electron density of the two atoms concerned. In the case of hydrogen, this does not coincide with its nuclear position, but is displaced significantly in the direction of the covalent bond (i.e., B—H). For example, O—H and N—H covalent bond lengths, which are observed to be 0.97 and 1.03 Å by neutron diffraction, can be determined to be as short as 0.6 and 0.7 Å, respectively, by X-ray diffraction (33). Hence, in order to identify an H-bond based on X-ray diffraction data, the H···A bond length should be at least 0.09 Å (34) shorter than the sum of the van der Waals radii (35) of H and A (36). Angular orientations are also of importance, viz. the extent of deviation from linearity of the A—H···B bond. Statistical surveys of H-bond geometry in small molecules have revealed a mean value close to 180° (37), although exceptions to this finding are plentiful and are often due to the geometric constraints imposed elsewhere in the structure.

In the solid state structure, an H-bond will form whenever it can because its formation will raise the stability of a molecular crystal by a few kilocalories per mole (38). The H$_3$PICTAME solid state structure nicely demonstrates this observation, with eight *intra*- and one *inter*molecular H-bonds per molecule. Following the nomenclature of H-bonding geometry, two types of such interactions are present in H$_3$PICTAME: two-center (chelate) and three-center (bifurcated) H-bonds (Fig. 2).

The atom labelling and numbering scheme used is shown in the ORTEP diagram of the X-ray crystal structure of H$_3$PICTAME (Fig. 3a). In each arm of the molecule, the arylamide moiety is held strictly planar (Fig. 3c) due to the extended π network of the aromatic amide linkage. The H-bond distances and some of the relevant bond angles are listed in Table 5, a perusal of which clearly indicates that all the H-bonds identified are well within the H···A distance criterion (H···O = 2.5 Å; H···N = 2.6 Å) and, as expected, the three-center H-bonds (H(5) H-bonded to N(3), N(4), and O(5) and H(6) H-bonded to N(5), N(6), and O(1), respectively) display a greater deviation from linearity.

Table 5. Hydrogen bonds (Å) and C—H···O interaction geometries (deg) in H$_3$PICTAME with estimated standard deviations in parentheses.

Interaction	D—H	H···A	D···A	D—H···A
O(2)—H(1)···O(1)[b]	0.96(3)	1.68(4)	2.565(3)	152(3)
O(4)—H(2)O(3)[b]	1.01(4)	1.65(4)	2.569(3)	148(3)
O(6)—H(3)O(5)[b]	1.29(5)	1.28(5)	2.575(3)	178(4)
N(1)—H(4)O(1)[a,b]	0.91	2.18	3.069(3)	164
N(1)—H(4)···N(2)[b]	0.91	2.29	2.689(3)	106
N(3)—H(5)···O(5)[c]	0.91	2.18	2.904(3)	136
N(3)—H(5)···N(4)[c]	0.91	2.29	2.690(3)	107
N(5)—H(6)···O(1)[c]	0.91	2.15	2.891(3)	138
N(5)—H(6)···N(6)[c]	0.91	2.27	2.682(3)	107
C(3)—H(11)···O(1)	0.98	2.51	2.824(3)	99
C(10)—H(16)···O(3)	0.98	2.49	2.842(3)	101
C(17)—H(20)···O(5)	0.98	2.51	2.827(3)	98

[a] Symmetry operation: ½ + x, −1/2 + y, 1 − z.
[b] Two centred H-bond.
[c] Three centred H-bond.

Fig. 2. The two types of H-bond present in the H$_3$PICTAME X-ray crystal structure.

two-center (chelate)   three-center (bifurcated)
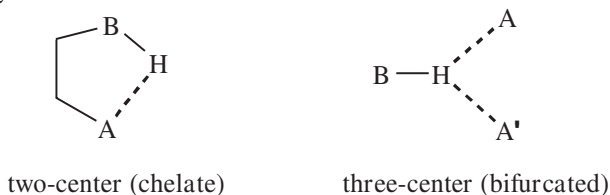
Fig. 3. (*a*) ORTEP representation of the X-ray crystal structure of H₃PICTAME; (*b*) torsion angles between amide nitrogens and apical C(2); (*c*) wire frame diagram showing only the three arylamide moieties with arrows representing the dihedral angles between the least-squares planes. In the wire framework representation, the arrangement and orientation of atoms are identical to that in (*a*). All values shown are based on the X-ray diffraction data; the planes include refined hydrogen atoms as well as all other non-hydrogen atoms of the arylamide moiety, but the backbone carbons are omitted for clarity.
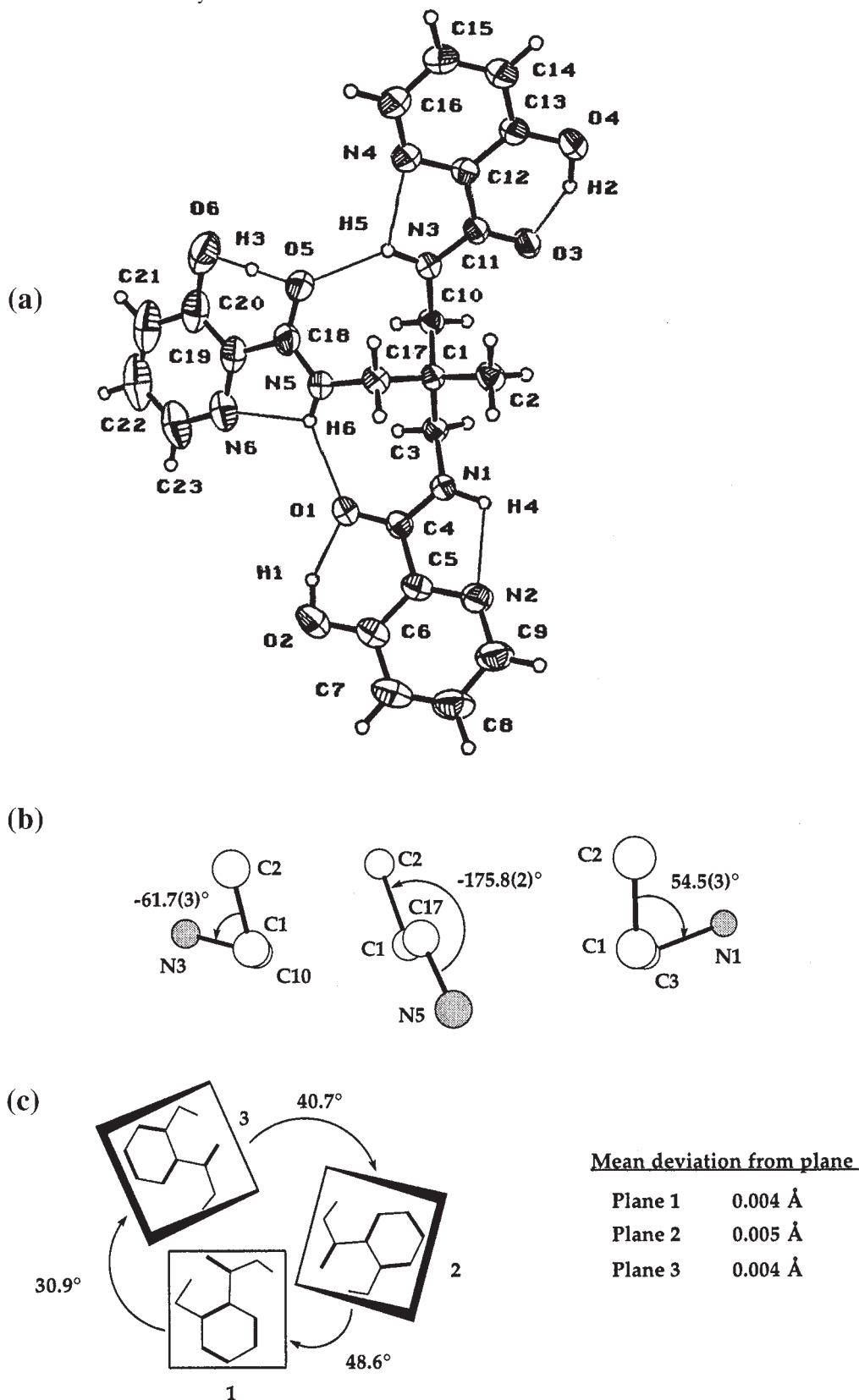
Table 6. pK_a values[a] of H$_3$NICTAME, H$_3$NICTREN, and related ligands (0.16 M NaCl, 25°C).

pK_a	H$_3$NICTAME	H$_3$NICTREN	H$_2$nic[e]	H$_2$pic[e]	H$_6$TRNS[f]	H$_6$TAMS[f]
1	10.68 (2)[b]	11.2 (2)[b]	11.99[b]	11.06[b]	11.2 (1)[c]	11.19 (4)[c]
2	10.58 (4)[b]	10.7 (2)[b]	4.98[d]	5.03[d]	10.6 (1)[c]	9.81 (4)[c]
3	9.71 (3)[b]	10.0 (1)[b]	< 0	< 0	9.59 (3)[c]	8.91 (2)[b]
4		6.25 (4)[c]			8.07 (3)[b]	7.95 (3)[b]
5					7.29 (3)[b]	6.56 (2)[b]
6					6.17 (3)[b]	2.92 (2)[c]

[a] The numbers in parentheses refer to 1σ.

[b] Phenol deprotonation.

[c] Ammonium deprotonation.

[d] Pyridinium deprotonation.

[e] Reference 44.

[f] Reference 45.

The molecule in the solid state lacks a C_3 axis of symmetry; the torsion angles about the apical C(2), the intervening methylene carbon, and the amidic nitrogen succinctly depict this fact (Fig. 3b). The apical carbon (C2) is in a staggered conformation with respect to N5; whereas the analogous torsion angles in the other two arms are roughly 60°, corresponding to a *gauche* conformation with one in a positive (clockwise) and the other in a negative (counterclockwise) sense. Since nearly all H-bond donors and acceptors are "buried" intramolecularly, preorganizing the molecule for chelation, only one *inter*molecular H-bond forms in each molecule as shown in Fig. 3. It is reasonable to conjecture, in the absence of an X-ray structure, that the structural isomer, H$_3$NICTAME, should show a greater propensity toward aggregation (as opposed to intramolecular H-bond formation) based merely on geometric considerations.

A noteworthy detail in the solid state H-bonding network present in H$_3$PICTAME is the variation in the H-bond distances (and angles) of the two-center O—H···O (Table 5). Thus, whereas O(6)—H(3)···O(5) constitutes a symmetrical H-bonding site, the other two analogous H-bonds are asymmetric and, accordingly, the corresponding H···O distances are significantly longer. The most interesting aspect about the geometry of the symmetrical site is that, as a result of its perfect linearity (within experimental error), an unseemly angle of 87(2)° is imposed upon the C(20)-O(6)-H(3) bond — in contrast to 105(2)° for the other two analogous angles (Fig. 3). In spite of this anomalous bond angle, however, the symmetrical disposition of the H3, with respect to the two adjacent oxygens (O6 and O5), is corroborated by the significant lengthening of the respective C(18)—O(5) bond to 1.254 Å, (C(4)—O(1) = 1.245 Å, C(11)—O(3) = 1.243 Å) and a decrease in the C(18)—N(5) bond to 1.324 Å (C(4)—N(1) = 1.327 Å, C(11)—N(3) = 1.333 Å). This observation would be expected if the amide resonance structure **ii** (Fig. 4) were more predominant; the more the type **ii** resonance contributes to the overall resonance hybrid structure, the better the H-bonding acceptor ability of that amidic oxygen. The structural data summarized above clearly reflect this fact: the concomitant increase in C=O and decrease in C—N bond lengths is paralleled by a shortening of the H-bond distance. Thus, not too surprisingly, the longest C=O bond length, C(18)—O(5), corresponds to the shortest H-bond (1.28(5) Å, O(5)···H(3)).

Fig. 4. The amide resonance and H-bonding (see text).
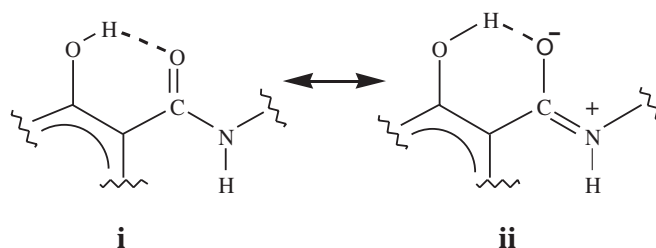
General characterization

The preorganization of a multidentate ligand is governed by two factors, each capable of diminishing the entropic penalty attendant upon metal ion complexation: (*i*) the conformation of each metal binding moiety in the molecule; (*ii*) the conformation of the "arms" (containing the binding moiety) with respect to each other. The first factor determines, for instance, the ease with which a chelate ring will form, while the second factor contributes to the complete encapsulation of the metal ion. Based on the solid state structure of H$_3$PICTAME, it is evident that although the structure is preorganized in the first sense, the three arms are not favorably disposed to define the cavity necessary for the coordination of a group 13 metal ion in a hexacoordinate octahedral polyhedron. In fact, in solution, as evinced by ^{1}H NMR spectroscopy, one set of signals is observed for the tripodal arylamides prepared, indicating that each arm rotates freely. The exceptions to this finding are, of course, H$_3$PICSPERM and H$_3$NICSPERM, which are asymmetric by virtue of their spermidine backbones. Therefore, for the purposes of solution coordination chemistry, the latter facet of preorganization is of no relevance in the case of the arylamides.

In considering the local conformation of each individual metal binding moiety, it is possible to predict which conformer is preferred (Fig. 5) by comparing the strengths of the hydrogen bonds available to the two forms. The strength of an H-bond (A—H···B) is known to depend on the relative acidity of A and the basicity of B; the strength of the H-bond should increase as the acid becomes more acidic and the base more basic (39). Since the phenolic hydrogens (pK_a ca. 10) (40) are more acidic than the amide (pK_a ca. 15) (41), the strongest H-bonds ought to occur in conformations **1a** and **2a** (Fig. 5). The ^{1}H NMR and IR spectroscopic results, although not unequivocally conclusive, appear to be in accord with the qualitative prediction that conformers **1a** and **2a** are prevalent in solution.

The ^{1}H NMR chemical shifts of the phenolic hydrogens of the arylamides show extensive downfield shifts (ca. 12 ppm in DMSO-d_6) indicative of H-bonding. The same observation was found to hold true in the less polar solvent CDCl$_3$, in the case of the picolinic amides; the nicotinic derivatives were not soluble enough in chloroform to allow for ^{1}H NMR spectroscopy (vide infra). On the other hand, the IR spectrum of H$_3$PICTAME in CCl$_4$ shows a broad band ranging from ca. 3200 to 2700 cm^{-1} characteristic of an intramolecular chelated phenolic OH stretching frequency (42). In the solid state IR spectrum of H$_3$PICTAME (KBr pellet), however, the phenolic stretching frequency ranges over a greater span from ca. 3600

Fig. 5. The two conformers of 3-hydroxypicolinyl (**1a**, **1b**) and 2-hydroxynicotinyl amide derivatives (**2a**, **2b**). (The dipole moments are depicted merely in a qualitative sense; they are not drawn to scale).

Observed water solubility trend: $1 < 2$
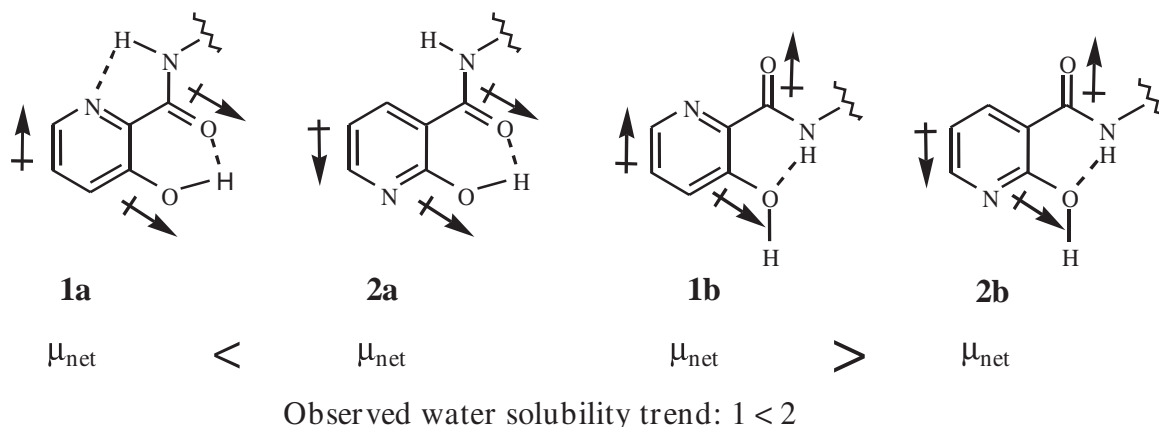
to 2700 cm^{-1}, in agreement with the solid state structure provided by X-ray crystallography wherein both intra- and intermolecular H-bonds are found to exist (the intermolecularly H-bonded OH stretching frequencies are found in the 3550–3450 cm^{-1} range) (42).

It is worthwhile to reflect on the significant solubility difference between the 2-hydroxynicotinyl and the 3-hydroxypicolinyl amide derivatives. The water solubility (at neutral pH) of the 3-hydroxypicolinyl amide derivatives is typically on the order of tens of μM as opposed to the 2-hydroxynictonyl counterparts that are soluble to the extent of ca. 0.5 mM, which is in accord with the polarity differences expected based on a qualitative consideration of dipole moments. In calculating the dipole moments of the molecule (μ_{net}) it is convenient to employ the moments of groups of atoms (amide, pyridine, OH) as an approximation (43) as shown in Fig. 5, where the magnitude of the three group moments are taken to be the same. It is clear that *only* type **a** conformers (Fig. 5) corroborate the observed water solubility trend.

The fact that 2-hydroxynicotinic amides adopt the type **2a** conformation is unexpected from the point of view of the electroneutrality principle (ref. 35, pp. 172 and 273), which would favor a conformation with a smaller electric dipole moment, i.e., the **2b** conformer. The reason for this conformational preference lies in H-bonding (cf. Fig. 5): the H-bonding in **2a** is more fortified, as discussed previously. Thus, the O—H···O hydrogen bond should still be stronger than N—H···O in water, even though this effect is mitigated in the presence of such a polar solvent; the H-bond energy decreases in more polar environments, since the H-bond has a substantial electrostatic component. Based on the evidence discussed here, the 2-hydroxynicotinic and the 3-hydroxypicolinic arylamides display an intramolecular H-bonding network that is sustained in water. Therefore, it can be concluded that these arylamide ligands are significantly partially preorganized for metal ion chelation.

Ligand deprotonation constants

The deprotonation constants[4] were obtained on the basis of a three- or four-proton model for H$_3$NICTAME and H$_3$NICTREN, respectively, in the pH 2.2–11.5 region at 25°C and in 0.16 M NaCl. The deprotonation constants thus obtained

appear in Table 6, and correspond to the successive deprotonation equilibria of the three phenols (pK_{a1}, pK_{a2}, pK_{a3}) and, in the case of H$_3$NICTREN, the deprotonation of the protonated apical nitrogen. The pK_a values of the pyridine ring nitrogens are too low to be measured in the pH range examined, while those of the amides fall outside the upper pH limit of the measurements. The water solubility of H$_3$PICTAME and H$_3$PICTREN was too low for potentiometric measurements.

It is appropriate to compare the pK_a's of H$_3$NICTAME and H$_3$NICTREN with those of the parent acids and some related aminephenol ligands (Table 6). The phenolic pK_a's of H$_3$NICTAME, H$_3$NICTREN, H$_2$nic, and H$_2$pic are particularly high. This would be anticipated for H$_3$NICTAME on the basis of its crystal structure, where all three phenol groups are involved in hydrogen bonding with the adjacent amide carbonyl oxygen. A similar explanation would account for the phenolic pK_a's of H$_3$NICTREN, and the high pK_{a1} of H$_2$nic and H$_2$pic is consistent with the presence of a six-membered H-bond ring involving the phenolic group and the deprotonated carboxylate oxygen of these ligands. These arguments are reinforced with the observation that for the aminephenols H$_6$TRNS and H$_6$TAMS, the phenolic pK_a's are much lower as there is no possibility of hydrogen bonding for the protonated phenol. In fact, the deprotonated phenolate oxygen may H-bond with an adjacent ammonium group, which would tend to favour deprotonation of the phenol and a low pK_a.

Concluding remarks

A series of potentially polydentate arylamide ligands have been synthesized from the coupling of several tripodal amines with nicotinic and picolinic acids and their derivatives. Two synthetic procedures were utilized in this study but the HO-SuNic method was not favoured due to the difficulty of separating the DCU side product from the activated ester. Hence, the CDI method was used in the synthesis of the compounds in this work.

The X-ray crystal structure of H$_3$PICTAME revealed extensive hydrogen bonding, with eight intra- and one

---

[4] The acid dissociation constant, K_a, is defined as:

$$H_nL^{m+} \rightleftharpoons H_{n-1}L^{(m-1)+} + H^+$$
$$K_{an} = ([H_{n-1}L^{(m-1)+}] [H^+]) / [H_nL^{m+}]$$
$$pK_a = -\log K_a$$

intermolecular H-bonds per molecule. In solution each arm of the tripodal arylamides rotates freely. Nevertheless, the NMR, IR, and solubility results indicate that the intramolecular H-bonding network of these arylamides is sustained in solution and, thus, these ligands are partially preorganized for the complexation of metal ions.

Acknowledgments

References

1. R.D. Shannon. Acta Crystallogr. Sect. A: Cryst. Phys. Diffr. Theor. Gen. Crystallogr. **A32**, 751 (1976).
2. F.A. Cotton and G. Wilkinson. Advanced inorganic chemistry. 4th ed. Wiley, Toronto. 1980. p. 682.
3. H. Kido and K. Saito. J. Am. Chem. Soc. **110**, 3187 (1980).
4. Struct. Bonding. **58**, (1984).
5. K.N. Raymond. Coord. Chem. Rev. **105**, 135 (1990).
6. S.M. Moerlien, M.J. Welch, K.N. Raymond, and F.L. Weitl. J. Nucl. Med. **22**, 720 (1982).
7. M.A. Green and M.J. Welch. J. Nucl. Med. Biol. **16**, 435 (1989).
8. T.B. Karpishin, T.M. Dewey, and K.N. Raymond. J. Am. Chem. Soc. **115**, 1842 (1993).
9. L.D. Loomis and K.N. Raymond. Inorg. Chem. **30**, 906 (1991).
10. K. Spartalian, W.R. Oosterhuis, and J.B. Neilands. J. Chem. Phys. **62**, 3538 (1975).
11. W.R. Harris, C.J. Carrano, S.R. Cooper, S.R. Sofen, A. Avdeef, J.V. McArdle, and K.N. Raymond. J. Am. Chem. Soc. **101**, 6097 (1979).
12. K.N. Raymond and C.J. Carrano. Acc. Chem. Res. **12**, 183 (1979).
13. W.R. Harris and K.N. Raymond. J. Am. Chem. Soc. **101**, 6534 (1979).
14. V.L. Pecoraro, W.R. Harris, G.B. Wong, C.J. Carrano, and K.N. Raymond. J. Am. Chem. Soc. **105**, 4623 (1983).
15. M.E. Cass, M. Garrett, and K.N. Raymond. J. Am. Chem. Soc. **111**, 1677 (1989).
16. M.M. Finnegan, S.J. Rettig, and C. Orvig. J. Am. Chem. Soc. **108**, 5033 (1986).
17. M. Finnegan, T.G. Lutz, W.O. Nelson, A. Smith, and C. Orvig. Inorg. Chem. **26**, 2171 (1987).
18. T.G. Lutz, D.J. Clevette, S.J. Rettig, and C. Orvig. Inorg. Chem. **28**, 715 (1989).
19. T.G. Lutz, D.J. Clevette, H.R. Hoveyda, V. Karunaratne, A. Nordin, S. Sjöberg, M.Winter, and C. Orvig. Can. J. Chem. **72**, 1362 (1994).
20. D. Kahne and W.C. Still. J. Am. Chem. Soc. **110**, 7529 (1988).
21. E.B. Fleischer, A.E. Gebala, A. Levey, and P.A. Tasker. J. Org. Chem. **36**, 3042 (1971).
22. W.C. Still, M. Kahn, and A. Mitra. J. Org. Chem. **43**, 2923 (1978).
23. F.E. Hahn and M. Tamm. Angew. Chem. Int. Ed. Engl. **30**, 203 (1991).
24. T. Miyazawa, T. Shimanouchi, and S.-I. Mizuchima. J. Chem. Phys. **24**, 408 (1956).
25. P. Caravan, T. Hedlund, S. Liu, S. Sjoberg, and C. Orvig. J. Am. Chem. Soc. **117**, 11230 (1995).
26. A.E. Martell and R.J. Motekaitis. Determination and use of stability constants. VCH, New York. 1988. p. 4.
27. *(a)* International tables for X-ray crystallography. Vol. IV. Kynoch Press, Birmingham, U.K. (present distributor Kluwer Academic Publishers: Boston, Mass., U.S.A.). 1974. pp. 99–102; *(b)* International tables for crystallography. Vol. C. Kluwer Academic Publishers, Boston, Mass., U.S.A. 1992. pp. 200–206.
28. G.W. Anderson, J.,E. Zimmerman and F.M. Callahan. J. Am. Chem. Soc. **86**, 1839 (1964).
29. J.C. Sheehan and G.P. Hess. J. Am. Chem. Soc. **77**, 1067 (1955).
30. A. Williams and I.T. Ibrahim. Chem. Rev. **81**, 589 (1981).
31. R. Paul and G.W. Anderson. J. Am. Chem. Soc. **82**, 4596 (1960).
32. H.A. Staab and W. Rohr. *In* Newer methods of preparative organic chemistry. *Edited by* W. Foerst. Academic, New York. 1968. pp. 72–74.
33. G.A. Jeffrey and W. Saenger. Hydrogen bonding in biological structures. Springer, Berlin. 1991. p. 108.
34. M.R. Churchill. Inorg. Chem. **12**, 1213 (1973).
35. L. Pauling. The nature of the chemical bond. 3rd ed. Cornell University Press, Ithaca, N.Y. 1960. p. 449.
36. W.C. Hamilton and J.A. Ibers. Hydrogen bonding in solids. Benjamin, New York. 1968. p. 14.
37. E.N. Baker and R.E. Hubbard. Prog. Biophys. Mol. Biol. **44**, 98 (1984), and references cited therein.
38. J. Donohue. J. Phys. Chem. **56**, 502 (1952).
39. T.M. Garrett, M.E. Cass, and K.N. Raymond. J. Coord. Chem. **25**, 241 (1992).
40. H.O. House. Modern synthetic reactions. 2nd ed. Benjamin, Menlo Park, N.J. 1972. p. 494.
41. H. Sigel and R.B. Martin. Chem. Rev. **82**, 385 (1982).
42. L.J. Bellamy. Infrared spectra of complex molecules. Vol. 1. 3rd ed. Chapman and Hall, New York. 1980. p. 108.
43. O. Exner. Dipole moments in organic chemistry. Georg Thieme, Stuttgart. 1975. pp. 30–34.
44. A.K. W. Stephens and C. Orvig. Inorg. Chim. Acta, **273**, 47 (1998).
45. P. Caravan and C. Orvig. Inorg. Chem. **36**, 236 (1997).